

# Impact of Waveform Segmentation Accuracy on Disturbance Recognition Reliability

M. Caujolle, M. Petit, G. Fleury, L. Berthet

**Abstract**— Power Quality disturbances can be identified by modern waveform analyzers using several recognition indicators. The indicators are computed after segmentation of the signal during either steady-state intervals or transient ones. This paper proposes indicators for the recognition of capacitor bank switching and transformer energizing events. These indicators computed over transient intervals prove to be robust to noise and harmonic disturbances. We also investigate their sensitivity to inaccurate detection instants. For each indicator, a validity interval is identified and its properties determined. Constraints on the segmentation stage are deduced from this analysis: a standard deviation less than 2.5 ms is required on the segmentation delay for reliable recognition of transformer energizing event, while a deviation less than 0.25 ms is necessary for capacitor switching recognition. For both event types, a near zero mean segmentation delay is to be expected.

**Keywords:** Disturbance, Segmentation, Recognition, Direction, Power Quality, Transformer energizing, Capacitor switching

## I. INTRODUCTION

With the increasing performance of the monitoring equipment connected to MV networks, advanced algorithms can be used to process the huge amount of measured waveforms in order to identify and locate power disturbances automatically. The usual recognition processes are made of two parts: the segmentation stage and the identification stage.

The segmentation stage provides the identification stage with temporal information about the measured disturbances by splitting the voltage and current waveforms into steady-state and transient intervals. In the literature, various indexes and related algorithms are proposed to do so [1]-[5].

A differentiated analysis of the waveforms is then carried out over the determined segments for identifying and locating events such as faults, transformer energizing or capacitor switching [1]-[2]. The set of indicators used for event characterization depends on the analyzed segment type. Mean electrotechnical quantities are used to define the steady-state behavior of the disturbance while transient indicators specify and quantify the fast variations observed. For the latter indicator type, the segmentation accuracy becomes a major concern as it directly impacts the reliability of the information they provide the recognition system with.

This paper proposes indicators for the identification and the relative location of events such as transformer energizing or capacitor switching. It also illustrates the impact of the segmentation accuracy on these indicators.

The structure of the used recognition system is outlined in Section II of this paper. Section III investigates the impact of segmentation accuracy on capacitor switching characterization and Section IV deals with its influence on transformer energizing event recognition. In these sections, values of the segmentation mean delay and standard deviation required for a reliable recognition of both event types are proposed.

## II. RECOGNITION SYSTEM STRUCTURE

### A. Segmentation Stage

#### 1) Segmentation process goals

The segmentation method used for waveform analysis splits them into transition and steady-state segments [2],[5]. The distinction between both interval types is based on the following concept:

- In normal operation or during lasting events, the measured waveforms display faint and slow changes. Whether disturbed or not, these segments are referred to as steady-state segments (in green in Fig. 1).
- The appearance or disappearance of PQ disturbances, such as faults, capacitor bank switching, transformer energizing..., lead to changes of the network operating point. These instants are materialized by significant and fast variations. The corresponding phases are referred to as transition segments (in red in Fig. 1).

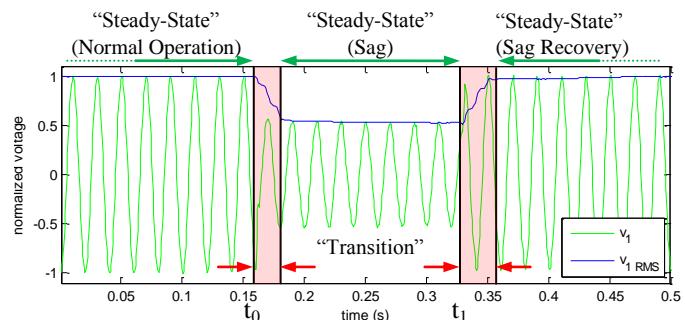


Fig. 1. Splitting of a disturbance into steady-state and transition segments. Appearance of a line-to-line fault at  $t_0 = 160$ ms, recovering at  $t_1 = 330$ ms. Shaded areas indicate the transition segments of the disturbance.

M. Caujolle and L. Berthet are with EDF R&D, Clamart, 92140 FRANCE (e-mail of corresponding author: mathieu.caujolle@supelec.fr).

M. Petit is with the Department of Power Energy Systems and G. Fleury is with the Department of Signal Processing & Electronic Systems, E3S – SUPELEC Systems Sciences, Gif-sur-Yvette, 91190 FRANCE.

Paper submitted to the International Conference on Power Systems Transients (IPST2011) in Delft, the Netherlands June 14-17, 2011

Segmentation quantities, such as the estimation error of harmonic models [3] and auto-regressive (AR) models [4], or the detail levels computed by Wavelet filter banks [1], can be used to distinguish the transitions from the waveform steady-states. Different methods are also found in the literature exploiting these indexes in order to detect the transitions.

Static thresholding [1],[3], noise adaptive [6] or spectral content adaptive [5] methods can be applied.

But, whatever the method, detection delay is unavoidable. To improve their accuracy, delay correction techniques may be applied after the signal analysis. In this case, the obtained detection time is either ahead the transient starting instant or delayed. It is to be noted that a precise analog event detection system was already used to reduce the detection latency in case of impulsive transients such as lightning strikes [19]-[20].

## 2) Segmentation assessing quantities

The previous segmentation methods provide various results in terms of reliability (percentage of missed and false detection) and accuracy (mean segmentation delay and standard deviation). The results given by the recognition stage are heavily influenced by those quantities. Disturbances can be misinterpreted because of missed or additional transitions, while erroneous values of recognition indicators can be computed because of early or delayed transition detection.

In this paper, two segmentation accuracy quantities are dealt with. The segmentation mean delay corresponds to the mean value of the time interval separating the detection time from the real transient starting instant. Depending on the segmentation method, it can be either positive or negative. The segmentation standard deviation informs about the width of the detection delay statistical distribution.

### B. Recognition stage

In the recognition stage, a decision system makes use of sets of indicators computed from the analyzed waveforms. These indicators give typical information about the detected disturbance. Either expert systems [17] or supervised learning methods [1],[13] can be used as decision system.

The waveform decomposition determined during the segmentation stage is required for the recognition indicator computation: different indicator sets are evaluated depending on the interval type. Mean values of typical electrotechnical quantities such as RMS values, symmetrical components or power are computed over steady-state intervals [17]. They are used to characterize faults or load switching events. For transient segment analysis, indicators studying either extremal variations or model parameters determined through pattern identification are used [1],[7],[13]. Events such as transformer energizing or capacitor bank switching are characterized by these indicators. Assessing transient behavior, the latter are more sensitive to segmentation accuracy.

In this paper, indicators used for identifying or locating transient events are proposed. The impact of detection delay on their reliability is investigated and tolerance levels are proposed for the two segmentation accuracy quantities.

## III. IMPACT ON CAPACITOR SWITCHING INDICATORS

### A. Characteristics of capacitor switching events

Shunt capacitors are extensively used in distribution networks as means of supplying reactive power to control system voltage, reduce equipment loading or improve its power factor. They are switched in and out as needed.

Capacitor switching operations thus frequently happen. These events produce transient oscillations on the voltage and current waveforms (Fig. 2.a). The transient characteristics mainly depend on the switched-in and in-service bank capacitances as well as on the upstream network impedance [14]. The primary transient frequency  $f_{c_1}$  (1) typically ranges between 300 and 1000 Hz.

$$f_{c_1} \approx \frac{1}{2\pi \sqrt{L_{upstream} \sum C_{bank}}} \quad (1)$$

Capacitor switching events being very short, most of the information is to be found in the very first instants of the disturbance. It consists of a set of damped sinusoidal oscillations that superimposes on the steady-state waveforms measured after the switching instant  $t_{sw}$ . In fact, characteristics such as the steady-state voltage and current amplitudes or the harmonic level are affected by capacitor switching. The variation magnitude depends on the size of the switched-in bank and on its position on the network [9]. The voltage and current waveforms can be modeled during the transient as a sum of  $N$  harmonics and  $M$  damped oscillations:

$$y(t) = \sum_{i=1}^N A_i \sin(\omega_0 h_i t + \varphi_i) + \sum_{i=1}^M A_{c_i} \sin(\omega_{c_i} t + \varphi_{c_i}) e^{-\alpha_{c_i}(t-t_{sw})} \quad (2)$$

### B. Sensitivity of Direction Indicators

Several direction indicators are found in the literature informing about the capacitor switching event direction. They analyze the behavior of the waveform just after the switching instant [8], the disturbance transient power and energy variations [10] or its spectral content [12].

#### 1) AH-filtered instantaneous power indicator computation

In this paper, we propose a new indicator derived from the one proposed in [8] and [9]. It relies on the same theoretical justification [9] but it proves to be more robust to noise and harmonic disturbances. It is also implementation friendlier. Its computation procedure consists of two steps.

A notch filter synchronized with the fundamental frequency is first applied to the measured voltage and current waveforms. It suppresses their steady-state fundamental and harmonic content (3). The modified zero crossing technique presented in [18] is used for its synchronization. This filter is referred to as an anti-harmonics filter (AHF). It enables the accurate extraction of the oscillatory transients produced by capacitor switching events and retains their initial spectral properties. A delay  $\tau$  equal to two fundamental periods  $T_0$  is used in order to limit the impact of the transition repetition observed on the filtered signals (Fig. 2.b).

$$h_v v_j(k) = v_j(k) - v_j(k - \tau) \quad (3)$$

Where:  $v_j(k)$  is either a sampled voltage  $v$  or current  $i$  waveform  $\tau$  is the filter delay ( $\tau = 2T_0$ )

In a second step, the instantaneous power ( $h_{s_j}$ ) of each pair of filtered voltage and current waveforms ( $h_v v_j, h_i i_j$ ) is computed (4). The obtained signal (Fig. 2.c) presents a  $2f_c$  oscillatory behavior and a higher damping factor.

$$h_{s_j}(k) = h_{v_j}(k) h_{i_j}(k) \quad (4)$$

By analyzing the sign of its first peak, we can determine the direction of the capacitor switching event. The resulting indicator  $peak\_h_{s_j}$  is used as follows:

- If  $peak\_h_{s_j} > 0$ , the capacitor bank is located upstream the measurement point.
- If  $peak\_h_{s_j} < 0$ , it is located downstream.

A 2/3 majority rule is used on the indicator determined for the three phases to finalize the direction estimation of the capacitor switching event.

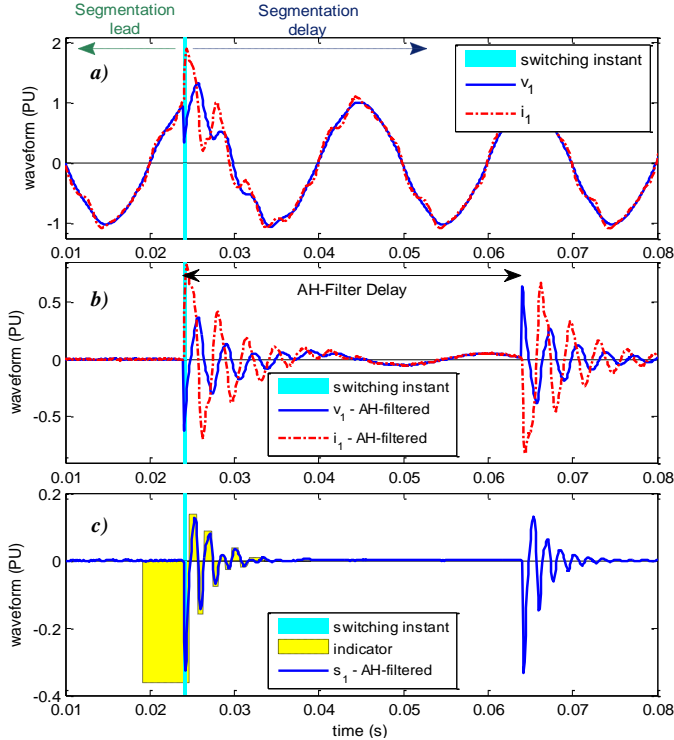


Fig. 2. Effect of capacitor bank switching; a) Measured voltage and current waveforms; b) Signals computed by an AHF; c) Computed instantaneous power and proposed direction indicator behavior depending on the detection instant (interval investigated  $t_{dect} \in [t_{sw}-T_0/2, t_{sw}+T_0]$ ).

The computation of this indicator requires the search of local maxima. If this method was applied directly to the voltage and current waveforms [8], it would be very sensitive to the signal harmonic and noise content. The prior application of the AH filter highly reduces the sensitivity of the local maximum search and simplifies its implementation. Moreover using the instantaneous energy of those signals rather than analyzing the filtered waveforms separately increases the damping and thus limits the impact of the secondary maxima.

## 2) Segmentation accuracy impact

If the proposed indicator works well under heavy noise and harmonic disturbances, its reliability still depends on the segmentation accuracy.

As shown in Fig. 2.c, the detection instant impacts its determined value. Two different areas are to be distinguished. For leading detection, the value given by the indicator is not affected. But, for delayed detection instants, the indicator shows an oscillatory pattern. Only a short time interval after

the switching instant still gives the required value.

In Fig. 3, the indicator evolution is displayed for different detection instants  $t_{dect}$  and main transient frequencies  $f_{c_1}$ . Other oscillation frequencies due to secondary network resonances are present in the signal but are not shown here.

Its analysis shows that the validity area of the proposed direction indicator consists of the early detection instant interval and of a limited time interval following the switching instant. Its size depends directly on the spectral content of the transient oscillation. The higher the oscillation frequency, the smaller the validity interval. Assuming a  $\pi/2$  phase shift between the voltage and current primary oscillations, relation (5) can be used to approximate the validity area size.

$$t_{validity} < t_{sw} + \frac{1}{8f_{c_1}} \quad (5)$$

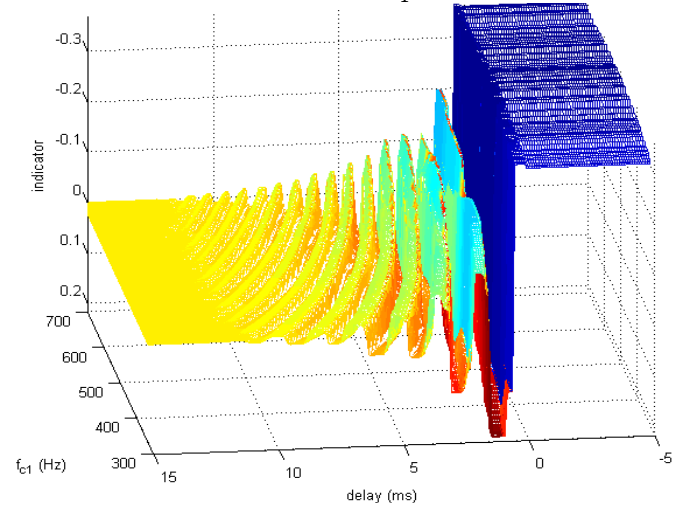


Fig. 3. Direction indicator behavior for different detection delays ( $t_{dect} - t_{sw}$ ) and primary oscillatory component frequencies  $f_{c_1} \in [300, 700]$  Hz

The safety interval upper bound is very restrictive as delays below 0.125 ms are required for 1 kHz transient frequencies. In presence of noise and harmonic disturbances, such accuracy is hardly achievable. In order to relax this constraint, the indicator implementation is adapted. We use the safe indicator behavior before the transient appearance instant and start to search for the local maximum a quarter-period ( $T_0/4$ ) before the detection instant. A sufficient margin is thus provided in case of both early and late detections and the constraint on the segmentation accuracy is redefined as follows (6).

$$t'_{validity} \leq t_{sw} + T_0/4 \quad (6)$$

It is to be noticed that the indicators proposed in [9] and [10] display similar sensitivity to segmentation instants. All of them rely on the local behavior of high frequency components.

## C. Sensitivity of Identification Indicators

A safe way to identify capacitor switching events from other transient disturbances is to estimate the characteristics of their spectral content. FFT transformation can be used to estimate the amplitudes and frequencies of the main components [2]. But this method has two drawbacks: limited resolution is provided because of the reduced signal observation window. It also lacks important information: the

damping factor that dissociates steady-state from transient components is not given.

### 1) Fitted model-based indicator computation

In this paper, we choose to estimate the signal component parameters using curve-fitting approach. To limit the order of the used signal model, the waveforms are first treated with the AHF previously described. This allows reducing the previous signal model (2) to its transient part. Here, we consider that a model consisting of a limited number ( $M = 3$ ) of oscillatory components (7) provides a sufficient approximation (Fig. 4).

$$v(t) = \sum_{i=1}^M A_{c_i} \sin(w_{c_i} t + \varphi_{c_i}) e^{-\alpha_{c_i}(t-t_{sw})} \quad (7)$$

The indicators used for the recognition of the disturbance are derived from the parameters estimated from the model: the amplitudes, the frequencies and the damping factors of the three main frequency components.

Statistical methods such as MUSIC or ESPRIT [15] could also be applied to determine the model parameter values. But, as only one observation of the signal is available, their accuracy and robustness remain limited.

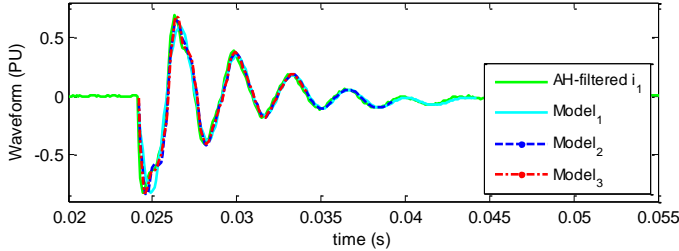


Fig. 4. Oscillatory models fitted to an AH-filtered current waveform

To provide robust estimation, we choose to fit the signal model to the transient waveform by solving a least square problem. Because of the typical model form, local minima are to be expected in the estimation error. In order to limit their influence, we use an iterative estimation scheme (Fig. 5).

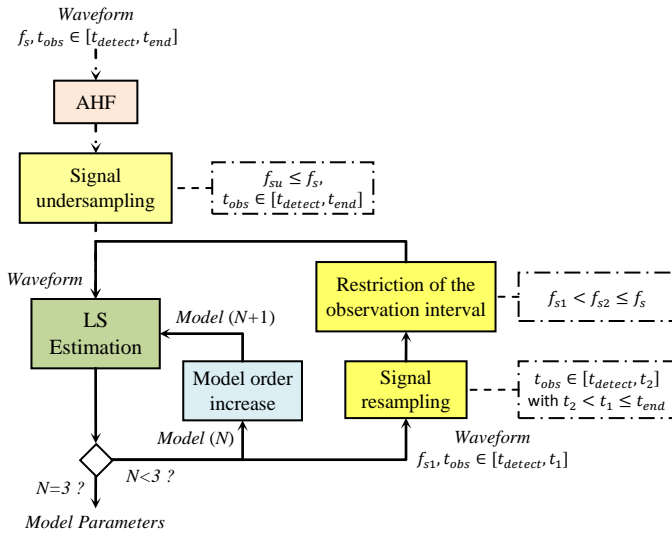


Fig. 5. Structure of the model parameter LS estimation process

At first, we undersample the AH-filtered waveforms. Then,

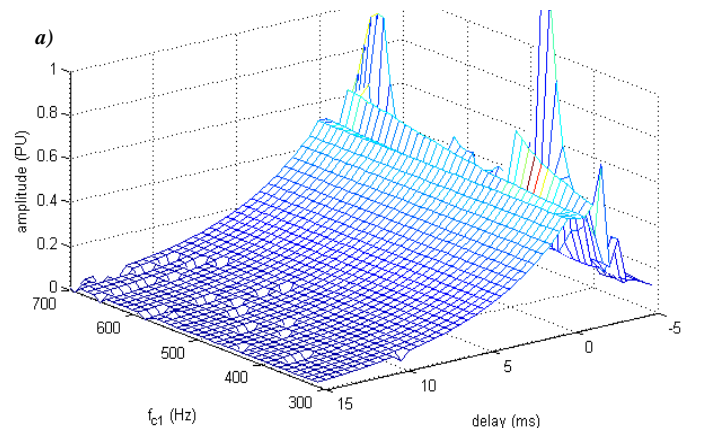
at each step, the model order is increased while the observation window is reduced and the signal sampling rate raised. By restricting the observation window size, we expect to improve the estimation accuracy of higher frequency components. The determined parameters values are used in the following iteration as initial values. This estimation structure is chosen because the higher spectral content of the transient is more damped. It is thus located during the very first instants following the switching time.

### 2) Segmentation accuracy impact

Thanks to the AHF pre-filtering and the iterative scheme, the estimation process proves to be very robust to noise and harmonic disturbances. But the determined parameters remain heavily dependent on the segmentation delay.

To evaluate the impact of this factor, we compute the disturbance amplitude, frequency and damping indicators for different detection delays and primary oscillations. As shown in Fig. 6, the estimation is little dependent on the disturbance spectral content. Four areas are distinguished according to the segmentation instant.

- For small detection delays, the amplitude is the only underestimated parameter. Both frequency and damping are correctly evaluated. This area size depends on the primary oscillation damping factor. The faster the attenuation, the shorter this area becomes.
- If the detection delay is too severe ( $>10$  ms), the estimation error quickly increases for all three parameters because of the lack of spectral information. In this area, sensitivity to noise becomes significant.
- The 10%-validity area is the interval around the switching instant on which the indicator estimation error is less than 10%. In case of delayed detection, its main limiting factor is the amplitude fast decrease during the instants following the switching (Fig. 6.a). In case of early detection, only a short interval provides valid values. For typical spectral content and damping factor, the validity area size can be approximated as follows:
$$t_{sw} - 0.5 \text{ ms} < t_{\text{validity}} < t_{sw} + 0.5 \text{ ms} \quad (8)$$
- For detection prior to this validity area, the evaluated damping factor and amplitude present important errors that render them unusable for identification.



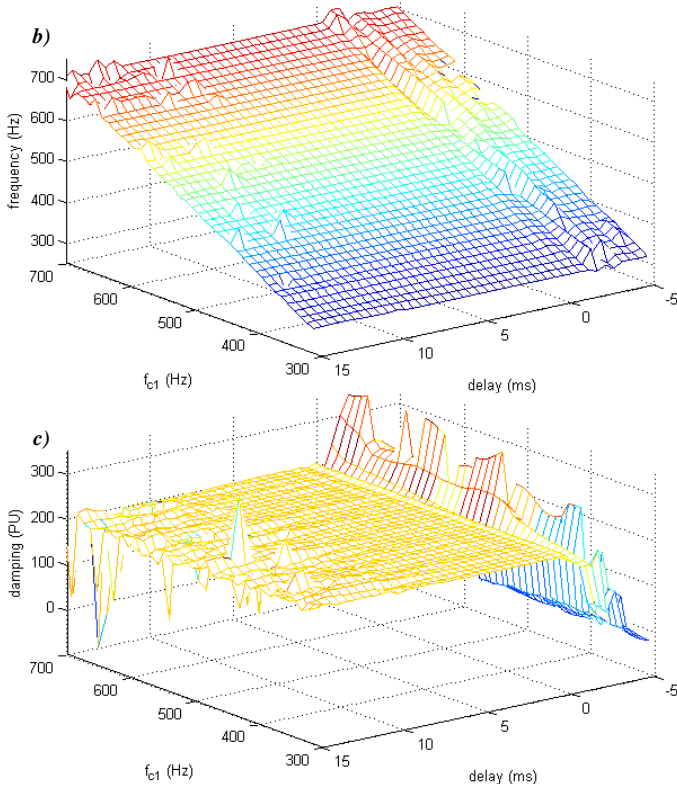


Fig. 6. Disturbance amplitude (a), frequency (b) and damping (c) indicators computed from the AH-filtered voltage waveform for different detection delays  $t_{detect} \in [t_{sw}-T_0/4, t_{sw}+3T_0/4]$  and primary oscillations  $f_{c1}$  between 300 and 700 Hz

#### D. Tolerance Levels for Capacitor Switching Events

The study of the indicators analyzing capacitor switching events shows a clear dependency between their reliability and the transient segmentation accuracy. The width of the validity area depends on the used indicator and its implementation way, but also on factors specific to the recorded disturbance.

To ensure sufficient reliability in capacitor bank switching recognition, the segmentation has to verify strict properties. While both indicator validity areas are different (6),(8), their intersection is symmetrical. A near zero mean segmentation delay has thus to be achieved by the decomposition algorithm. For switching transient primary frequency ranging between 300 Hz and 1 kHz, a standard deviation smaller than 0.25 ms, has to be reached to achieve over 95% reliability.

### IV. IMPACT ON TRANSFORMER ENERGIZING INDICATORS

#### A. Characteristics of Transformer Energizing Events

Transformer and feeder energizing are common events on MV networks. They usually occur during network recovery phases after protection system operation.

These disturbances display typical features. During the recovery stage, the voltage and current waveform amplitudes follow a quasi-exponential behavior (Fig. 7). Moreover, because of the saturation of the switched-in transformer magnetic cores, high levels of even harmonics are present in the waveforms [2]. These components decrease and disappear when the new steady-state is reached.

#### B. Sensitivity of half-cycle RMS Value based Indicator

##### 1) Half-cycle RMS value based indicator computation

Several recognition indicators are based on the presence of high even harmonic levels during the energizing events. One way to make use of this feature is to analyze the voltage and current half-cycle RMS values (Fig. 7). These quantities display an oscillatory behavior in presence of even harmonic components [16].

In this paper, we investigate the indicator proposed in [1]. It is based on the percentage of recovered voltage within a one-cycle analysis window. The indicator  $D$  is computed from the normalized minimum ( $V_m$ ) and maximum ( $V_p$ ) values of the half-cycle RMS voltage observed during the first cycle following the detection time of the disturbance (9). Supposing an accurate detection (detection time equal to appearance time), the corresponding points are displayed in Fig. 7.a.

$$D = \frac{V_p - V_m}{1 - V_m} \quad \text{where: } \begin{cases} V_p = \max_{[t_0, t_0+T_0]} V_{RMS-T_0/2} \\ V_m = \min_{[t_0, t_0+T_0]} V_{RMS-T_0/2} \end{cases} \quad (9)$$

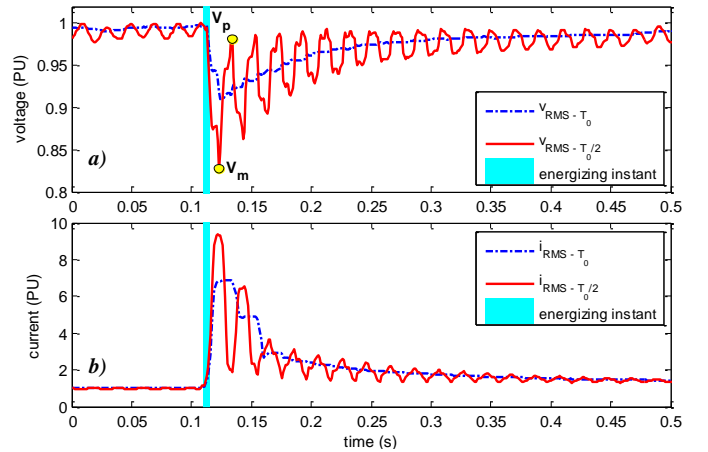


Fig. 7. Behavior of the voltage (a) and current (b) RMS values over one-cycle and half-cycle sliding-windows during a transformer energizing event

##### 2) Segmentation accuracy impact

In case of an ideal segmentation, the characteristic points  $V_p$  and  $V_m$  defining the half-cycle RMS based indicator (9) are located around constant positions. They should respectively be reached about a half-cycle and a cycle after the detection time. Thus, the theoretical indicator validity area at least ranges between 0 and a half-cycle ( $T_0/2$ ) after the energizing instant.

Fig. 8 displays the behavior of the recovered voltage based indicator for detection instants between  $t_{sw}-4T_0$  and  $t_{sw}+10T_0$ . Before as well as after the energizing instant, the indicator values remain in the expected range defined in [1], that is  $D > 0.5$  in case of transformer energizing. In steady-state, the indicator shows large computational instability because of the proximity of the lower and upper envelopes (Fig. 8). It is quite sensitive to noise and steady-state changes because of the voltage magnitude normalization. In specific situations, indicator values above one could even be achieved.

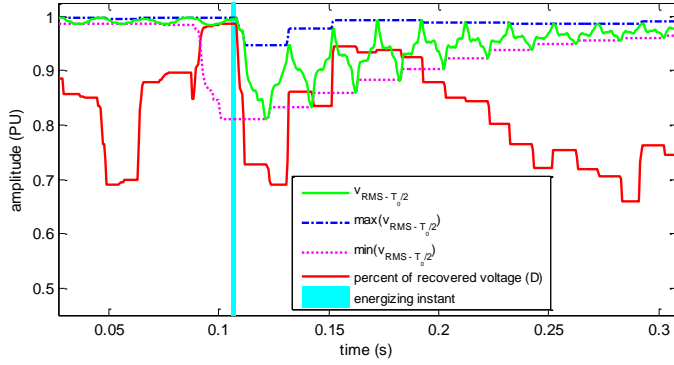


Fig. 8. Recovered voltage based indicator [1] during transformer energizing.

Because of this behavior, no validity area can be defined. As shown in [7], this indicator may be used to discriminate fault transitions from transformer energizing events. But it cannot ensure the presence of transformer energizing: in case of false segmentation, it always indicates non-existing transformer energizing events.

### C. Sensitivity of Fitted-Model Based Indicators

#### 1) Exponential fitted-model based indicator computation

In this part, we propose another type of recognition indicators. They are based on the parameters of simple exponential models (10) followed by the voltage and current RMS values during the switching event (Fig. 9).

For the voltage, the exponential model consists of the switching variation  $v_{jump}$ , the steady-state value of the amplitude during the new steady-state  $v_{ss}$  and the recovery coefficient  $\alpha$ . For the current, we rather choose to study the behavior of its variation. Thus, the model constant parameter corresponds to the current variation observed between the two surrounding steady-states  $\Delta i_{ss}$ . The exponential behavior as well as the used model parameters is outlined in Fig. 9.

$$\begin{cases} v(t) = v_{ss} - v_{jump}e^{-\alpha(t-t_{detect})} \\ \Delta i(t) = \Delta i_{ss} + i_{jump}e^{-\beta(t-t_{detect})} \end{cases} \quad (10)$$

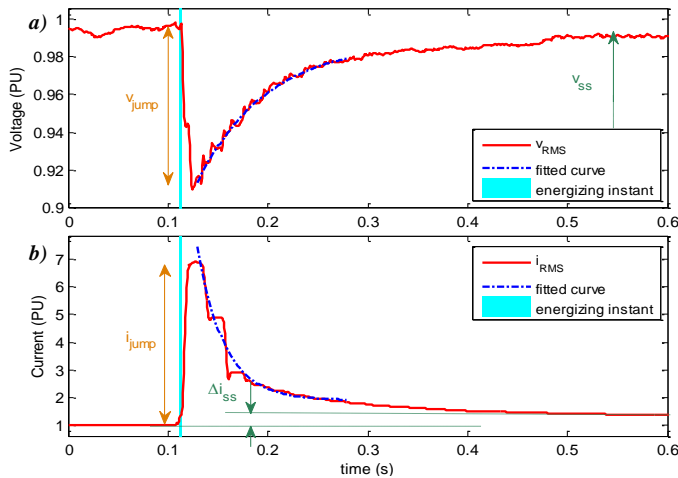


Fig. 9. Exponential models fitted to voltage (a) and current (b) RMS values.

As seen in Fig. 9, the voltage and current one-cycle RMS values do not present a clear jump at the switching instant. It takes one period to reach their maximum value. This time

interval corresponds to the response time of the RMS calculus. It is not taken into account by the fitting process since it may distort the evaluation. The analysis interval considered by the model estimation process has to start one period after the disturbance detection instant.

While the computation of the indicators proposed for capacitor switching recognition requires the use of a specific estimation procedure, a typical LS estimation is used in this case. The lower model complexity eases the identification process.

#### 2) Segmentation accuracy impact

The computed indicators determined from exponential model parameters are little dependent on noise and harmonic disturbances since they are fitted to one-cycle RMS values. They are however impacted by the event detection instants.

In Fig. 10, the indicator behavior is displayed for different detection instants.

- In case of detection earlier than a half period before the energizing event, huge errors appear on the estimated indicators. These errors come from the growing importance of the steep magnitude variation observed during the first period following the transition appearance.
- After the event appearance, the indicator behavior is steadier, but the estimation error progressively increases with the detection delay.
- The 10%-validity area of the indicators is limited to an interval centered on the disturbance appearance instant. Its width depends little on transformer energizing characteristics such as the sag depth and the damping factor (Fig. 11). It is more dependent on the RMS value time response. Relation (11) can be used to approximate the validity area for usual energizing events.

$$t_{sw} - T_0/4 < t_{validity} < t_{sw} + T_0/4 \quad (11)$$

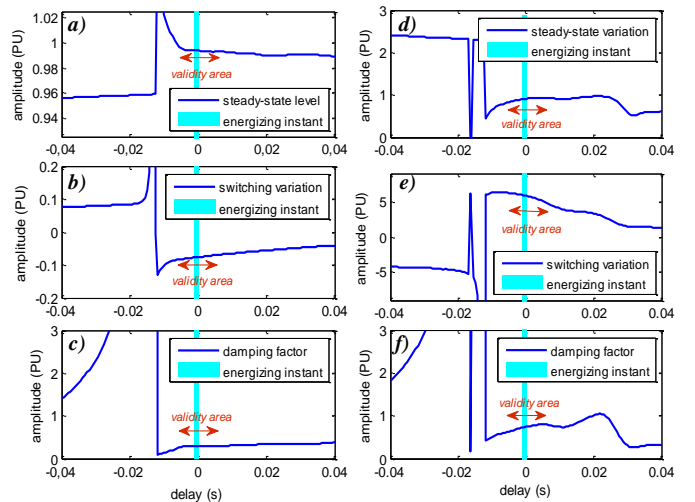


Fig. 10. Exponential model-based recognition indicator behavior for detection instants between  $t_{detect} \in [t_{sw} - 2T_0, t_{sw} + 2T_0]$

Voltage: steady-state level (a), switching variation (b) and damping (c)  
Current: steady-state variation (d), switching variation (e) and damping (f)

The analysis of Fig. 11 also shows that the current indicator behavior is less regular than the voltage one. This irregularity

comes from the step-like behavior of the current RMS values during the first periods following the disturbance appearance (Fig. 9.b). Depending on the step width taken in consideration by the estimation process, the damping factor and amplitudes increase or decrease slightly.

#### D. Tolerance Levels for Transformer Energizing Events

Segmentation delay induces different behaviors depending on the used indicator. For the half-cycle RMS based indicator proposed in [1], no influence is noticed since it is unable to distinguish steady-states from transformer energizing events. But, for the indicators determined by exponential model curve-fitting, a 10%-validity area can clearly be established. This restricted time interval is symmetrical and limited on both sides of the detection instant (11). Its width little depends on the transformer energizing event characteristics.

So, to limit the indicator estimation error, the waveform segmentation has to provide a near zero mean segmentation delay. For typical sag amplitudes, a standard deviation smaller than  $T_0/8$ , that is 2.5 ms, has also to be reached to allow reliable indicator estimation.

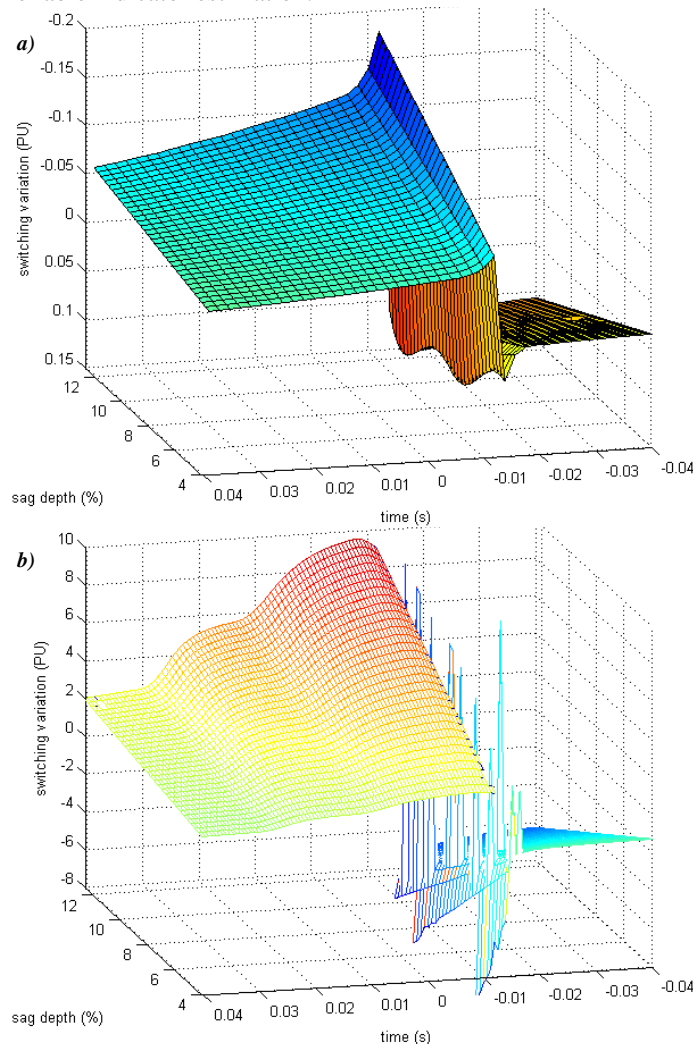


Fig. 11. Switching variation indicator  $vi_{jump}$  behavior for voltage (a) and current (b). Detection instants between  $t_{detect} \in [t_{sw}-2T_0, t_{sw}+2T_0]$  and sag depth between 4 and 15% are investigated.

## V. CONCLUSIONS

Several identification and direction indicators are presented in this paper. These are dedicated to either transformer energizing or capacitor switching events recognition.

For ideal segmentation, the curve-fitting based recognition indicators as well as the AH-filtered power one proved to be robust to noise and harmonic disturbances. Each of them is dedicated to a single disturbance type for which it analyses specific features. This allows them to be very discriminating.

Despite their robustness, the proposed indicators still depend on the transient detection instants. Several factors, such as the event amplitude or the frequency range, impact their validity area.

For most indicators used for transformer energizing characterization, the impact on the indicator values remains small when segmentation errors smaller than a quarter of period are observed. For such events, the required mean segmentation delay has to be near zero and the allowed standard deviation smaller than 2.5 ms.

For capacitor switching, higher segmentation accuracy is required. The validity areas of most indicators used for their identification and direction discrimination depend on the main transient frequency. In this case, the mean delay must also be near zero, while the required standard deviation has to be much smaller. A value of 0.25 ms is suggested.

For safe capacitor switching indicator computation, strict conditions have to be achieved by the segmentation process. This is possible using detection algorithms and delay compensation methods little sensitive to noise and harmonic disturbances with high sampled signals ( $f_s > 10\text{kHz}$ ). Since the accuracy constraints are less severe for transformer energizing indicators, they are reached more easily. In this case, lower sampled signals ( $f_s \sim 2\text{kHz}$ ) can be used.

Future work will involve investigating processes for PQ disturbance segmentation. Recognition systems using several identification and location indicator types will also be studied.

## VI. REFERENCES

- [1] S. Santoso, W.M. Grady, E.J. Powers, J. Lamoree, "Characterization of Distribution Power Quality Events with Fourier and Wavelet Transforms", *IEEE Trans on Power Delivery*, vol. 15, n°1, January 2000
- [2] M.H.J. Bollen, I.Y.H. Gu, "Signal Processing of Power Quality Disturbances", Wiley&Sons, 2006
- [3] E. Styvaktakis, "Automating power quality analysis", *PhD, Chalmers University of Technology, Sweden, 2002.*
- [4] I.Y.H. Gu, M.H.J. Bollen, E. Styvaktakis, "The Use of Time-Varying AR Models for the Characterization of Voltage Disturbances", *Power Engineering Society Winter Meeting, IEEE, 2000*
- [5] M. Caujolle, M. Petit, G. Fleury, L. Berthet, "Reliable Power Disturbance Detection using Wavelet Decomposition or Harmonic Model based Kalman Filtering", *ICHQP Proceedings, Sept. 2010*
- [6] J. Chung, E.J. Powers, W.M. Grady, S.C. Bhatt, "New robust voltage sag disturbance detector using and adaptive prediction error filter", *IEEE Power Engineering Society Summer Meeting, 1999*

- [7] I.Y.H. Gu, N. Ernberg, E. Styvaktakis, "A Statistical-Based Sequential Method for Fast Online Detection of Fault-Induced Voltage Dips", *IEEE Trans. on Power Delivery*, vol. 10, n°2, pp. 497-504, April 2004.
- [8] K.Hur, S.Santoso, "On two Fundamental Signatures for determining the Relative Location of Switched Capacitor Banks", *IEEE Trans. on Power Delivery*, vol. 23, n°2, April 2008.
- [9] S.Santoso, "On Determining the Relative Location of Switched Capacitor Banks", *IEEE Trans. on Power Delivery*, vol. 22, n°2, April 2007.
- [10] A.C.Parson, W.M.Grady, E.J.Powers, J.C.Soward, "Rules for Locating the Sources of Capacitor Switching Disturbances", *Power Engineering Society Summer Meeting*, IEEE, 1999
- [11] A.C.Parson, W.M.Grady, E.J.Powers, J.C.Soward, "A Direction Finder for Power Quality Disturbances Based Upon Disturbance Power and Energy", *IEEE Trans. on Power Delivery*, vol. 15 n°3, July 2000.
- [12] Y.-J. Shin, E.J. Powers, W.M. Grady. A. Arapostathis, "Signal Processing-Based Direction Finder for Transient Capacitor Switching Disturbances", *IEEE Trans. on Power Delivery*, vol.23, n°4, October 2008.
- [13] S. Santoso., E. J. Powers, W. M. Grady, "Power Quality Disturbance Waveform Recognition Using Wavelet-Based Neural Classifier", *IEEE Trans. on Power Delivery*, vol.15, n°1, January 2000
- [14] R. Natarajan, *Power System Capacitors*, Taylor&Francis, 2005
- [15] I.Y.H. Gu, M.H.J. Bollen, "Estimating Interharmonics by Using Sliding-Window ESPRIT", *IEEE Trans. on Power Delivery*, vol.23 n°1, 2008
- [16] F. Wang, M.H.J. Bollen, "Frequency-Response Characteristics and Error Estimation in RMS Measurement", *IEEE Trans. on Power Delivery*, vol. 19 n°4, October 2004
- [17] Math H. J. Bollen, "Algorithms for Characterizing Measured Three-Phase Unbalanced Voltage Dips", *IEEE Trans. on Power Delivery*, vol 18, n°3, July 2003.
- [18] M.M. Begovic, P.M. Djuric, S. Dunlap, A.G. Phadke, "Frequency Tracking in Power Networks in the Poresence of Harmonics", *IEEE Trans. on Power Delivery*, vol. 8, n°2, July 1993.
- [19] L. Peretto, P. Rinaldi, R. Sasdelli, R. Tinarelli, A. Fioravanti, "Implementation and Characterization of a System for the Evaluation of the Starting Instant of Lightning-Induced Transients", *IEEE Trans. on Instrumentation and Measurement*, Vol. 56-5, Oct. 2007, pp. 1955-1960
- [20] K. Yamabuki, A. Borghetti, F. Napolitano, C.A. Nucci, M. Paolone, L. Peretto, R. Tinarelli, M. Bernardi, R. Vitale, "A Distributed Measurement System for Correlating Faults to Lightning in Distribution Networks", *Proc. of the International Symposium on High Voltage Engineering (ISH)*, Aug. 27-31, 2007